SUPER-RESOLUTION/SEGMENTATION OF 3D TRABECULAR BONE IMAGES WITH TOTAL VARIATION AND NONCONVEX CAHN-HILLIARD FUNCTIONAL

Yufei Li[1], *Bruno Sixou*[1], *Andrew Burghardt*[2], *Françoise Peyrin*[1,3]

[1] CREATIS, CNRS UMR 5220, Inserm U630, INSA de Lyon, Universite de Lyon, F-69621

[2] Musculoskeletal Quantitative Imaging Research Group, Department of Radiology and Biomedical Imaging, University of California, San Francisco, CA, 94158, USA

[3] ESRF,6 rue Jules Horovitz, F-38043, Grenoble Cedex France

ABSTRACT

The analysis of trabecular bone micro structure from *in-vivo* CT images is still limited due to insufficient spatial resolution. In a previous work, we have investigated the use of super resolution techniques to improve image quality based on a TV based approach. However, the method is limited to recover the bimodal nature of the image. In this work, we investigate the use of a double well non convex constraint to solve the joint super resolution/segmentation problem. Two different minimization schemes are proposed to obtain a critical point of the non convex functional. The two methods improve the reconstruction results on real data.

Index Terms— Super-resolution/segmentation, nonconvex, nonsmooth, Cahn Hilliard, total variation, 3D CT image, bone micro-architecture.

1. INTRODUCTION

The study of the trabecular bone micro-architecture is crucial in the diagnosis of osteoporosis because it is one of the determinant of bone strength [1]. New High Resolution peripheral Quantitative CT (HR-pQCT) devices with improved spatial resolution are now available to investigate the bone micro-architecture with *in-vivo* [2] measurements.

The bone structure analysis is based on the segmentation of the images to extract the bone from background. This segmentation is the first step to calculate morphological or topological parameters describing the bone micro-structure. Yet, the segmentation step remains an issue because the spatial resolution of the images is still too low compared with the trabeculae bone size.

The aim of this work is to investigate joint super-resolution and segmentation methods to improve the trabecular bone analysis from *in-vivo* HR-pQCT images. In previous works, we investigated methods to improve the quality of trabecular bone micro-CT images based on Total Variation regularization [3, 4]. The images we considered having a quasi-binary structure, good results were obtained with single-image super-resolution. Results on experimental micro-CT images artificially deteriorated showed an improvement of the bone parameters. However, the effect of convex constraint used in our TV regularization method remains limited to recover the bimodal histogram of the ground truth image.

In this work, we propose to investigate the addition of a double well non convex constraint to the TV regularized functional in view to enhance the bimodality of the estimated image. A good candidate is the Cahn-Hilliard model [5] which is characterized by a double-well potential. This functional is difficult to minimize but numerical methods adapted to this type of non-convex functional have been investigated [6–8]. On the other hand, nonconvex and nonsmooth problems have received much attention nowadays in signal and image processing. Recently, different approaches have been proposed to find critical points for non convex and non differentiable functionals based on proximal operators [9], iterative reweighted algorithms [10] or the Alternating Direction Method of Multipliers (ADMM).

Our main objective here is to compare two minimization schemes for the regularization functional. This paper is organized as follows. In the second section, we introduce the joint segmentation/super-resolution inverse problem and the Cahn-Hilliard model. Two different methods to minimize the regularization functional will be described in section 3. In section 4, we present numerical results based on HR-pQCT images of bone samples. Conclusion and perspective work will be presented in section 5.

2. SUPER-RESOLUTION/SEGMENTATION PROBLEM WITH TV AND CAHN-HILLIARD DOUBLE WELL POTENTIAL

2.1. The inverse problem formulation

The reconstruction of a 3D image with an improved resolution from a single low-resolution image is based on the direct problem of the image degradation. In our approach, we assume that the low-resolution image is obtained from a high-resolution image with blur, down sampling and noise. The forward problem can be written as:

$$g = Af + n \tag{1}$$

where $g \in \mathbb{R}^N$ denotes the N-voxels 3D low-resolution noisy image, and $f \in \mathbb{R}^{N'}$ denotes an $N' = N \times p^3$-voxels 3D high-resolution image with super-resolution factor $p = 2$ in each dimension, $A : \mathbb{R}^N \subset L_2(\Omega) \to \mathbb{R}^{N'} \subset L_2(\Omega)$ is the linear operator accounting for blurring followed by down-sampling defined on the bounded domain Ω and n is the noise component. Our inverse problem is to recover the image f from the given degraded image g. We assume the blurring

kernel is known from preliminary measurements. It is an ill-posed problem, errors in the data will be magnified and this problem must be regularized. Stable solutions can be obtained by minimizing a regularization functional of the form:

$$J(f) = \min_f \|Af - g^\delta\|_2^2 + \mu\mathcal{R}(f) \quad (2)$$

where $\mathcal{R}(f)$ is a regularization term introducing some *a priori* knowledge on the solution. The first term enforces the fitting to the data. The regularization parameter μ controls the balance between the two terms of the regularization functional.

The images considered are quasi-binary and the problem can be understood as a joint segmentation/reconstruction problem. Recently, we investigated Total Variation(TV) schemes as a regularization term to solve this problem to obtain stable solutions [3]. The TV regularization term is defined as $TV(f) = \int_\Omega |\nabla f(\mathbf{r})| d\mathbf{r}$, where $|\nabla f(\mathbf{r})|$ is the Euclidean norm of the gradient. As a well-known way to recover edges of an image, the TV is also easy to minimize because of its convexity. However, other non convex regularizers can be investigated to enforce the quasi binary nature of the image.

2.2. Double well potential Cahn-Hilliard model

The double well potential of Cahn-Hilliard model for binary images is defined by $W(f) = f^2(1-f)^2$. A class of fourth order inpainting algorithms for binary images using a modified Cahn-Hilliard equation has been proposed by Bertozzi, Esedoglu and Gilette [7, 8] considering convexity methods with the Sobolev H^{-1} gradient and the inner product $\langle ., . \rangle_{-1} = \langle \nabla\triangle^{-1}, \nabla\triangle^{-1} \rangle$. In this work, we consider the potential $W(f) = (f-f_1)^2(f-f_2)^2$, where f_1 and f_2 are the positions of two peaks of the histogram. We will consider the following minimization problem including the TV term and the Cahn-Hilliard term:

$$J(f) = \min_f \|Af - g^\delta\|_2^2 + \mu_1 TV(f) + \mu_2 W(f) \quad (3)$$

μ_1 and μ_2 have a balancing effects for regularization terms.

3. TWO DIFFERENT NONCONVEX OPTIMIZATION ALGORITHMS

In this section, we present two different algorithms for non-smooth and nonconvex minimization. The first one is based on the method for nonconvex and nonsmooth minimization with linear constraints presented in [11]. The second one is a combination of the ADMM scheme with the minimization method of the Cahn-Hilliard potential presented in [7].

3.1. Linearly constrained nonsmooth and nonconvex minimization method(LCNNM)

The principle of the algorithm is to add a sequence of quadratic perturbations to the non convex functional to build a strongly convex functional. In order to use the algorithm proposed in [11], we define the following functionals:

$$J(f) = ||Af - g||^2 + \mu_2 \sum_i W(f)$$

$$J_{\omega,v}(f) = J(f) + \mu_2\omega||f - v||^2$$

For the double well potential, the constant $\omega = \frac{1}{2}(\frac{f_1+f_2}{2})^2 + 1$ is chosen such that $J_{\omega,v}$ is ν-strongly convex. Then we define the following convex functional with linear constraints:

$$\overline{J}_{\omega,v}(f,u) = J_{\omega,v}(f) + \mu_1 \sum_i ||u_i|| \qquad \text{s.t. } Df = u$$

with $Df = (D_x f, D_y f, D_z f)_i$. The sum is extended to the voxel i. In order to take into account the linear constraint an augmented Lagrangien is considered with a Lagrangien parameter λ. A saddle point of the Lagrangien is obtained with optimization with respect to the primal and dual variables. The method and the convergence properties are detailed in [11].

3.2. An ADMM approach for the minimization with the H^{-1} minimization

The existence of a solution for the Cahn-Hilliard potential and the image inpainting was proven in the framework of the H^{-1} Sobolev spaces in [5, 7, 12]. Here we apply ADMM to combine the double well potential $W(f)$ and TV. One difference with respect to the previous algorithm is that $W(f)$ will be minimized by H^{-1} gradient. This method will be denoted CH+TV in the following.

Taking into account the linear constraints, the augmented Lagrangian can be formulated as:

$$\begin{aligned}\mathcal{L}_A = \frac{1}{2}||Af - g||_2^2 + \mu_1 \sum_i \{||h_i|| + \frac{\beta}{2}||h_i - D_i f||^2 \\ - \lambda_i^t(h_i - D_i f)\} + \mu_2\{\sum_i \frac{1}{\varepsilon}W(s) + \varepsilon||\nabla s||^2 \\ + \frac{\beta}{2}||s - f||_2^2 - \lambda_D^t(s - f)\}\end{aligned}$$

h_i and s are splitting variables and λ_i and λ_D are Lagrangian multipliers for TV and double well functions respectively. The saddle point of the Lagrangian is obtained with successive updates:

1. update of $f^{(k+1)}$

$$\begin{aligned}(A^tA + \mu_1 \sum_i \beta D_i^t D_i + \mu_2\beta I)f = A^t g \\ + \mu_1 \sum_i (\beta D_i^t h_i^{(k)} - D_i^t \lambda_i^{(k)}) + \mu_2(\beta s^{(k)} - \lambda_D^{(k)})\end{aligned}$$

   The solution of this linear equation was obtained with a conjugate gradient method.

2. update of $h_i^{(k+1)}$: $h_i^{(k+1)} = S_\beta(D_i f^{(k+1)} + \lambda_i^{(k)}/\beta)$ where $S_\beta(u) = max(1 - \frac{1}{\beta|u| + \epsilon}, 0) \cdot u$. Here ϵ is a small number ensuring the stability of algorithm in case that $|u| \simeq 0$.

3. update of $s^{(k+1)}$, here we use the approach of Esedoglu et al.

$$\begin{aligned}s^{(k+1)} + \triangle t(\varepsilon\triangle^2 s^{(k+1)} - C_1\triangle s^{(k+1)} + C_2 s^{(k+1)}) = \\ \triangle t(\triangle(\frac{1}{\varepsilon}W'(s^{(k)})) + \beta(f^{(k+1)} - s) + \lambda_D \\ - C_1\triangle s^{(k)} + C_2 s^{(k)}) + s^{(k)}\end{aligned}$$

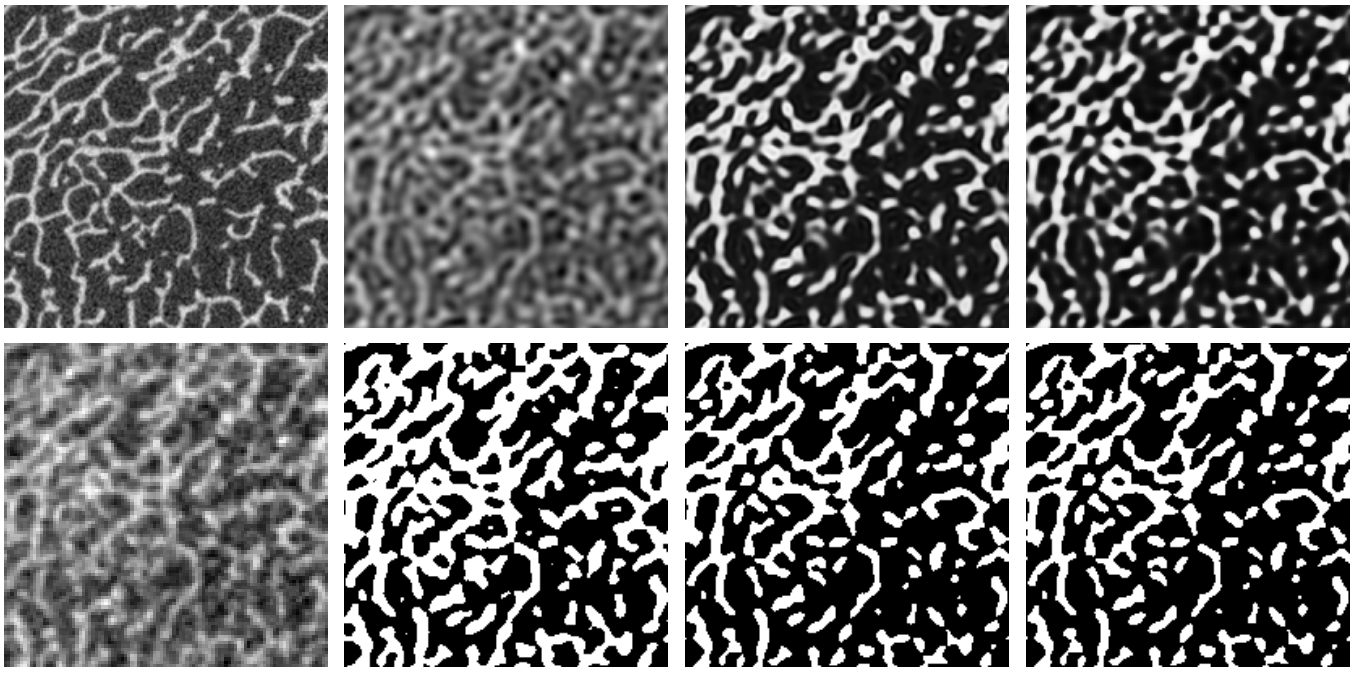

Fig. 1: first column: images from μCT (first row), HR-pQCT (second row); second column: TV optimization for HR-pQCT image, binarized TV optimization; third column: CH+TV results from TV gray level estimation, binarized CH+TV optimization results; fourth column: LCNNM results based on TV gray level estimation and binarized LCNNM results.

where $\triangle t$ is time step length. Following the work on [6, 7], the solution was obtained with Fourier transforms. The constants C_1, C_2 and ε are chosen to ensure the convergence of the algorithm.

4. update of $\lambda_i^{(k+1)}$ and $\lambda_D^{(k+1)}$

$$\lambda_i^{(k+1)} = \lambda_i^{(k)} - \beta(h_i^{(k+1)} - D_i f^{(k+1)})$$
$$\lambda_D^{(k+1)} = \lambda_D^{(k)} - \beta(s^{(k+1)} - f^{(k+1)})$$

4. NUMERICAL EXPERIMENTS

4.1. Simulation details

The tests were performed on experimental images of trabecular bone obtained from HR-pQCT [2] and micro-CT. We regard the images from HR-pQCT as low resolution images with a resolution $82\mu m$; the images from micro-CT as high resolution image, with a resolution equal to $41\mu m$. After registration, the size of cropped ROI (region of interest) are 100x100x100 and 200x200x200 respectively. A first TV reconstruction is performed as a starting point for the two minimization schemes.

For each iteration, the PSNR, Dice and the BV/TV ratio are calculated. The grey level image is segmented with Otsu method [13], projected on the average values of the segmented regions to obtain an image with two discrete levels f_b. The data term is estimated by $||Af_b - g||_2^2$. The first algorithm has been demonstrated to reach a stationary point. The second algorithm is stopped at the minimum of the former data term.

4.2. Results

Fig.1 shows the high and low resolution images, the gray level and binary images reconstructed with the TV regularization, with the TV and Cahn-Hilliard regularization terms with the two minimization schemes, LCNNM and CH+TV. Figures 2, 3 and 4 illustrate the evolution of the PSNR, of the Dice (Dice $= \dfrac{2f_{br} \cdot f_b^*}{f_{br} + f_b^*}$, f_{br} is the binarized reconstruction image, f_b^* is the binarized high resolution image), of the BV/TV (ratio of bone volume to total volume) and of the data term evaluated on the binary image with the iterations for the two minimization schemes. The reconstruction results are improved with the nonconvex penalty and the two minimization methods. Fig.2 3 illustrate that CH+TV and LCNNM lead to similar Dice index if the CH+TV iterations are stopped at the minima of the data term as shown on Fig.5. The divergence of the data term for CH+TV might be related to the nonconvexity of the regularization functional. The convergence is guaranteed for LCNNM. Moreover, the reconstruction results with CH+TV are better regarding the BV/TV.

5. CONCLUSION

In this paper, we proposed to use a non convex functional based on the Cahn-Hilliard double well potential to improve the segmentation/super-resolution results obtained with the TV regularization on HR-pQCT images. Two different minimization schemes are proposed. The Dice as well as the BV/TV were improved by the two methods. We will validate CH+TV algorithm for a larger range of images with various bone densities.

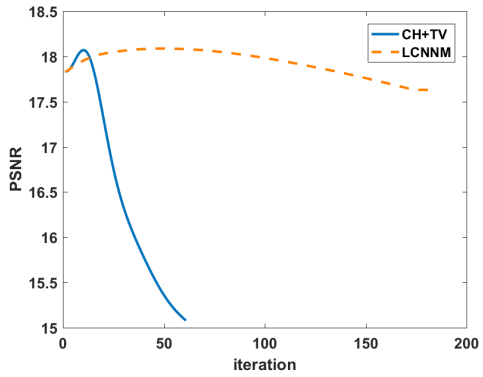

Fig. 2: Evolution of PSNR criterion as a function of the iteration number for the two algorithms.

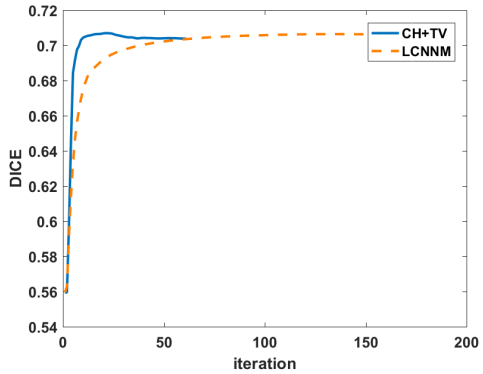

Fig. 3: Evolution of DICE criterion as a function of the iteration number for the two algorithms.

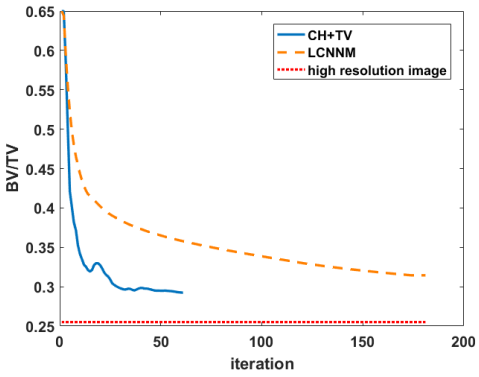

Fig. 4: Evolution of BV/TV criterion as a function of the iteration number for the two algorithms.

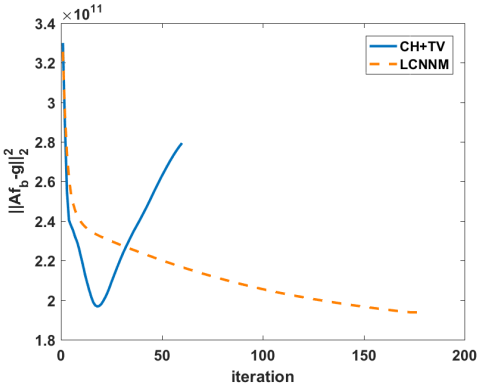

Fig. 5: Evolution of $||Af_b - g||_2^2$ criterion as a function of the iteration number for the two algorithms.

6. REFERENCES

[1] Ego Seeman and Pierre D Delmas, "Bone qualitythe material and structural basis of bone strength and fragility," *New England Journal of Medicine*, vol. 354, no. 21, pp. 2250–2261, 2006.

[2] Stephanie Boutroy, Mary L Bouxsein, Françoise Munoz, and Pierre D Delmas, "In vivo assessment of trabecular bone microarchitecture by high-resolution peripheral quantitative computed tomography," *The Journal of Clinical Endocrinology & Metabolism*, vol. 90, no. 12, pp. 6508–6515, 2005.

[3] Alina Toma, Loïc Denis, Bruno Sixou, Jean-Baptiste Pialat, and Françoise Peyrin, "Total variation super-resolution for 3D trabecular bone micro-structure segmentation," in *2014 22nd European Signal Processing Conference (EUSIPCO)*. IEEE, 2014, pp. 2220–2224.

[4] Alina Toma, Bruno Sixou, and Françoise Peyrin, "Iterative choice of the optimal regularization parameter in TV image restoration.," *Inverse Problems & Imaging*, vol. 9, no. 4, 2015.

[5] Charles M Elliott, "The Cahn-Hilliard model for the kinetics of phase separation," in *Mathematical models for phase change problems*, pp. 35–73. Springer, 1989.

[6] David J Eyre, "An unconditionally stable one-step scheme for gradient systems," *Unpublished article*, 1998.

[7] Andrea L Bertozzi, Selim Esedoḡlu, and Alan Gillette, "Inpainting of binary images using the Cahn-Hilliard equation," *IEEE Transactions on image processing*, vol. 16, no. 1, pp. 285–291, 2007.

[8] Andrea Bertozzi, Selim Esedoḡlu, and Alan Gillette, "Analysis of a two-scale Cahn-Hilliard model for binary image inpainting," *Multiscale Modeling & Simulation*, vol. 6, no. 3, pp. 913–936, 2007.

[9] Huan Li and Zhouchen Lin, "Accelerated proximal gradient methods for nonconvex programming," in *Advances in Neural Information Processing Systems*, 2015, pp. 379–387.

[10] Emmanuel J Candes, Michael B Wakin, and Stephen P Boyd, "Enhancing sparsity by reweighted l_1 minimization," *Journal of Fourier analysis and applications*, vol. 14, no. 5-6, pp. 877–905, 2008.

[11] Marco Artina, Massimo Fornasier, and Francesco Solombrino, "Linearly constrained nonsmooth and nonconvex minimization," *SIAM Journal on Optimization*, vol. 23, no. 3, pp. 1904–1937, 2013.

[12] Martin Burger, Lin He, and Carola-Bibiane Schönlieb, "Cahn-hilliard inpainting and a generalization for grayvalue images," *SIAM Journal on Imaging Sciences*, vol. 2, no. 4, pp. 1129–1167, 2009.

[13] Nobuyuki Otsu, "A threshold selection method from gray-level histograms," *Automatica*, vol. 11, no. 285-296, pp. 23–27, 1975.